Preprints.org

Article

Not peer-reviewed version

Microstructural Analysis of Hyaluronic Acid-Zinc Oxide Nanoparticle Composite Films: Investigation of Phase Separation and Interfacial Compatibility

Kolawole S. Dada *, Falia F. Zaripova, Roman O. Olekhnovich

Posted Date: 10 November 2025

doi: 10.20944/preprints202511.0609.v1

Keywords: polymer; composite film; ZnO NPs; hyaluronic acid; interphase compatibility; phase separation; surface morphology; polymer-nanoparticle interaction

Preprints.org is a free multidisciplinary platform providing preprint service that is dedicated to making early versions of research outputs permanently available and citable. Preprints posted at Preprints.org appear in Web of Science, Crossref, Google Scholar, Scilit, Europe PMC.

Copyright: This open access article is published under a Creative Commons CC BY 4.0 license, which permit the free download, distribution, and reuse, provided that the author and preprint are cited in any reuse.

Preprints.org (www.preprints.org) | NOT PEER-REVIEWED | Posted: 10 November 2025 doi:10.20944/preprints202511.0609.v1

Disclaimer/Publisher's Note: The statements, opinions, and data contained in all publications are solely those of the individual author(s) and contributor(s) and not of MDPI and/or the editor(s). MDPI and/or the editor(s) disclaim responsibility for any injury to people or property resulting from any ideas, methods, instructions, or products referred to in the content.

Article

Microstructural Analysis of Hyaluronic Acid-Zinc Oxide Nanoparticle Composite Films: Investigation of Phase Separation and Interfacial Compatibility

Kolawole S. Dada [1,*], Falia F. Zaripova [1] and Roman O. Olekhnovich [2]

[1] Chemical Engineering Center, ITMO University, Saint Petersburg, Rusia Federation

[2] ITMO University, Saint Petersburg, Rusia Federation

* Correspondence: dada.kolawole@niuitmo.ru; Tel.: +79939581531

Abstract

Microstructure of composite films composed of polymers and nanoparticles is crucial for understanding the nanoparticles (NPs) dispersion and the role by colloidal stability played in the film formation process. The research aims to create composite films from the combination of hyaluronic acid (HA) and zinc oxide nanoparticles (ZnO NPs) to produce materials that integrate antimicrobial properties as a medical application interface. The main problem of composite films involving ZnO NPs is dispersion in polymer matrix which compromises mechanical integrity and structure performance. We discovered key parameters of phase separation influenced by thermodynamic factors and then observed interfacial compatibility through a nanoscale resolution ZnO NPs dispersion, its adhesion mechanisms and defect distribution. We utilized a pH driven HA/ZnO electrostatic reaction by generating a protonation without any form of chemical change, using citric acid as stabilizing agent and this reverses the Zeta potential of the filler (ZnO NPs) to +25mV , and then we used atomic force microscopy (AFM) to study the microstructure of the films and optical microscope for the morphology. The process also covers surface modification of ZnO through PEGylation. The AFM analysis showed that surface roughness and particle size vary with respect to whether the ZnO nanoparticles were functionalized, unmodified or chelated. The research results will help create HA-based composite films and microneedles with specific nanostructures for wound healing and drug delivery administration.

Keywords: polymer; composite film; ZnO NPs; hyaluronic acid; interphase compatibility; phase separation; surface morphology; polymer-nanoparticle interaction

1. Introduction

Hyaluronic acid (HA) is a naturally found polysaccharide that has emerged in research and is very significant due to its properties, such as biocompatibility, hydrophilicity and its modulation ability in tissue repair [1,2] This thoroughly marks its importance in biomedical applications. Consideration of a synergistic integration of HA-ZnO NPs , there is a formulation result of films/patches used for the administration of drug delivery, wound dressing and cell differentiation when acting as a scaffold [3].There are challenges based on flaws in total dispersion ,which could result in agglomeration and thereby results in non-uniform across the surface area [4] .These could be due to factors defined by phase separation and this redefines it interfacial compatibility. These can be responsible for structural integrity, drug kinetic release, antimicrobial properties functionality [5].

The dynamics of the interfacial relationship between the composite (HA-ZnO NPs) is necessary to define its stress transfer, mechanical support, stability in colloidal solutions, dispersion and binding concepts [6]. The concept of interfacial bonding expressively modulates the final structure formation. Studying the effect of Weak interactive VanderWaal forces, which may result in poor adhesion, while the likes of covalent or hydrogen can increase integration.

© 2025 by the author(s). Distributed under a Creative Commons CC BY license.

Preprints.org (www.preprints.org) | NOT PEER-REVIEWED | Posted: 10 November 2025 doi:10.20944/preprints202511.0609.v1

In Elaborating on the Physical and chemical characteristics of HA,it is a naturally occurring polysaccharide that reflects an array of physical and chemical characteristics required for different applications [7].There are various ranges of molecular weight,which demonstrates its viscosity and mechanical strength capacity [8]. HA demonstrates a very good water solubility which is also dependents on pH and temperature exposure to form a stable aqueous solution across all physiological range [9,10]

The other property of HA in-terms of its behaviour ,display a non-Newtonian phase of shear thinning characteristics under applied mechanical stress [11,12] ,which forms gel like networks at higher concentrations.Its thermal stability is also as a result of its amorphous crystallization with semi-crystalline domains.This polymer exhibits a high frequency of transparency in aqueous solutions with limited UV absorption.There is also a known property of HA, which is its hydrophilic nature with high surface energy that attracts water interaction which helps to support cell interaction [13].This materials is also significant as it exhibits a defined paths of glass transition temperature and specific degradation temperature range for defining its stability.

However, from the chemical spheres, HA has a structure that is characterized by three functional groups which are the hydroxyl(-OH), carboxyl (-COOH), and lastly the N-acetyl groups [14,15].The hydroxyl groups is responsible for hydrogen bonding and helps for water solubility process, the carboxyl group is responsible for pH-response character and ionization. Lastly, the N-acetyl group helps to stabilize the molecular structure and its also a determining factor for biological activity.

More-so, the molecular structure of HA , consists of repeating disaccharide units which are linked by glycosidic bonds, which then forms helical chain conformations that creates complex molecular networks.The polymer has a modification ability into esterification reactions which helps to create a cross linking modification and can metamorphosize into various chemical derivations.This modification potential of HA makes it possible to utilize in various performance functions and applications.This makes HA a versatile material for various application in biomedical and industrial uses [16–18]

Zinc oxide nano particles (ZnO NPs) is very distinctive in its attributes of physical properties, which makes them very useful in composite formation. They have a crystalline structure which exhibits a hexagonal wurtzite shape. ZnO NPs exhibits mechanical strength and hardness and a high young modulus which contributes to its reinforcement properties and capabilities [19]

The chemical properties of ZnO NPs is also highly important. It has a high surface energy with affinity for strong interfacial interactions with other polymer matrices. [20,21]The surface area is compounded by zinc and oxygen ions, which participates in various chemical reactions and interactions.They also show an evidence of amphoteric behaviour which shows potentials to react with both acids and bases. [22,23]

ZnO NPs is ideally selected to be used as a filler in this film formation, due to its several distinctive properties that make them suitable for use in HA composites film formation in drug delivery [24] which includes its high surface area-to-volume ratio, possession of a band gap of 3.37 eV, and an exciton binding energy of 60 MeV [25]. The Food Drug Administration (FDA) has always classified ZnO nanoparticles as "GRAS" (generally considered safe), and they show superior biocompatibility compared to other metal oxides, improved antimicrobial properties, and strong anti-inflammatory effects. [26,27]

Moreso, other several alternative nonmetal oxides have been investigated through research for HA composites film formation [28–30], which includes silicon dioxide nanoparticles, which provide excellent biocompatibility and a large surface area too but they exhibit lower antimicrobial activity and lower UV protection compared to ZnO [31,32]. Carbon-based nanomaterials that provide high mechanical strength and excellent electrical conductivity have also been investigated, although they cause potential toxicity and require higher production costs [33,34].

In a recent research as published, Figure 1 the phase behavior of HA-ZnO composite materials shows a complex interphase between polymer chains and the nano particle fillers .There is a reflection of multiphase morphology which shows separated region rich in HA and ZnO-rich region, varying

© 2025 by the author(s). Distributed under a Creative Commons CC BY license.

Preprints.org (www.preprints.org) | NOT PEER-REVIEWED | Posted: 10 November 2025 doi:10.20944/preprints202511.0609.v1

film thickness across film surface and mechanical instability [35] This is a function of thermodynamic principles where , the overall phase seperation patterns are determined by both the enthalpic and entropic factors.These are supported by models of theoretical origins and practical observations which includes the Flory-Huggins theory of polymer solution and DLVO theory of nano particles colloidal stability.There are factors responsible for the separation in the composite dynamics.Several researches has pointed out molecular weight, where higher molecular weight chains establishes an increase chain entanglements and reduced mobility.The concentration of ZnO nanoparticles can also affect the process of seperation.At higher concentration ,there is a tendency for wider phase seperation which is caused by particle size interactions other known factors are film preparation techniques based on variables like preparation temperatures, mixing speeds, drying temperature and so on.

The total interaction potential is defined as:

$V_T(r) = V_{vdW}(r) + V_{el}(r)$

Table 1. Interfacial compatibility of ZnO-HA pH-modulated conditions.

Parameter	ZnO Nanoparticles (ZnO NPs)	Hyaluronic acid (HA)	Interfacial/phase Behavior
Surface charge (pH-dependent)	Surface charges varies with pH, becomes positive in acidic and negative in basic media	Naturally negatively charges due to carboxyl and hydroxyl groups	Controlled pH adjustment aligns ZnO with HA, enhancing electrostatic compatibility
Dispersion Behavior	Poor dispersion when surface charge is near neutral (aggregation)	Acts as a stabilizing polymeric matrix	Optimal pH yields uniform ZnO dispersion within HA matrix
Interparticle Interaction	DVLO forces dominate (van der Waals attraction, electrostatic repulsion)	Adds non DVLO steric and hydration stabilization	Balanced DVLO non DVLO forces suppress aggregation and prevent phase separation
Resulting Phase Stability	Instability or phase separation at unadjusted pH	Stable hybrid network when ZnO-HA charge interactions are complementary	pH-modulated charge control leads to improved interfacial compatibility and film uniformity

© 2025 by the author(s). Distributed under a Creative Commons CC BY license.

Preprints.org (www.preprints.org) | NOT PEER-REVIEWED | Posted: 10 November 2025 doi:10.20944/preprints202511.0609.v1

Figure 1. shows the resultant film formation for (A) without modification and (B) after modification.

During the research, to better understand the phase interface transition process, some characterization methods were simply utilized, because using traditional characterization methods usually fall short in solving nano scale features, Optical Microscope and Atomic force microscope (AFM), FTIR These supports better visualization of the resulting physical properties of HA-ZnO micro-structures on a high chemical resolution tendency. Correspondence imaging approaches combine surface texture data with elemental mapping. These offers a multidimensional area on phase distribution, nano particles dispersion and inter-facial defects.

The Objective of this research is to identify the micro-structural detailed signatures of phase separation in the composite material of HA-ZnO. studying the quantifying effect of inter-facial compatibility through a process of nano scale imaging. The objective is to also stabilize a process guideline to bypass flaws in structural formation, using the parameters at optimal values. This research will establish a rational design of HA-based composites designed towards fulfillment of usage in bio-medicals, cosmetics and other environmental administration. The future of HA-ZnO NP composites seems promising, as current research is focused on optimizing synthesis methods and exploring new applications, making them particularly valuable for biomedical applications due to their unique combination of biocompatibility, antimicrobial properties, and mechanical reinforcement.

2. Methodology and Material

2.1. Materials

Hyaluronate (HA, MW ~ 1000kDa), was provided by Huaxi Biotechnology Co., Ltd. (Shandong, China), Zinc Oxide Nanoparticles / Nano powder (ZnO) 99.8% purity of size 10-30 nm was prepared at the center for chemical engineering center laboratory, ITMO University. The ultrapure water was prepared in the laboratory and used for the preparation of all aqueous solutions.

© 2025 by the author(s). Distributed under a Creative Commons CC BY license.

Preprints.org (www.preprints.org) | NOT PEER-REVIEWED | Posted: 10 November 2025 doi:10.20944/preprints202511.0609.v1

2.2. Methods

2.2.1. Preparation of Composite of HA-ZnO Films

The preparation of HA-ZnO NP composite films began with an accurate wt. measurement .0.2 % hyaluronic acid of Higher molecular weight (HMW) 1000kDa using a Mettler Toledo XP205 analytical balance, which was then dissolved in distilled water under careful stirring at temperature of 45 ± 1°C and kept stirred for 45minutes as in Figure 2 (A). ZnO nanoparticles were prepared by dispersing 0-10% by weight relative to HA in distilled water, followed by ultrasonic treatment for 45 minutes using a Branson 3510 ultrasonic bath to ensure uniform dispersion as seen in Figure 2 (B). The pH of the ZnO NP dispersion was adjusted to 5.65 ± 0.05 from 7.6 (average) as seen in Fig2 below, using 0.1 M citric acid, after which it was added by pipetting to the HA solution and stirred for 24 hours at room temperature using a Heidolph RZR 2021 top-drive agitator. Another sample of ZnO was PEGylated at controlled concentration of 10% using 0.1M of NaOH to increase the pH of ZnO to 10-11 from 7.6 (average).The composite mixture was then cast on a clean glass substrate and subjected to UV curing using a CL-1000L UV crosslinking agent with a wavelength of 365 nm for 15 minutes, followed by drying at room temperature of 23 ± 1°C for 4 days, during which the temperature and humidity were constantly monitored using a humidity and temperature sensor Vaisala HMT330.

Figure 2. The process of formation of the transdermal patch: the magnetic stirrer (2A), the dispersion of the ZnO using ultrasound bath (2B), formed films (2C) .

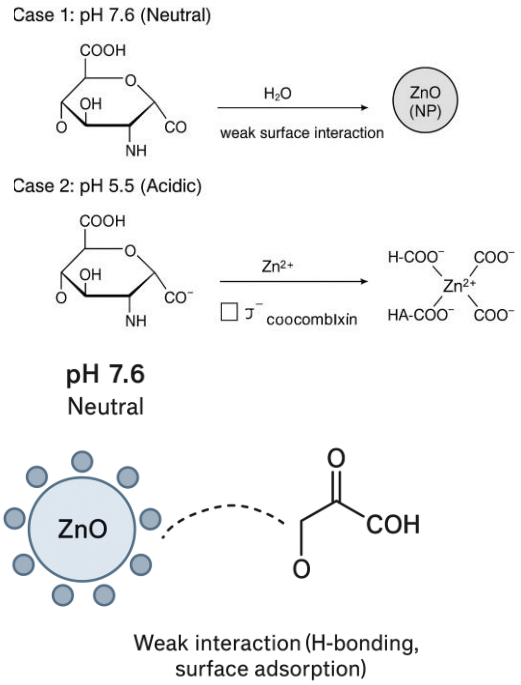

Figure 3. shows difference in reaction of film formation for HA-ZnO based on pH variance. When pH is measured at 5.5 for ZnO.

© 2025 by the author(s). Distributed under a Creative Commons CC BY license.

Preprints.org (www.preprints.org) | NOT PEER-REVIEWED | Posted: 10 November 2025 doi:10.20944/preprints202511.0609.v1

2.3. Characterization Techniques

2.3.1. Atomic Force Microscope (AFM)

The composite film surface topography and nanoparticle dispersion were analyzed using an AFM model in tapping mode. The obtained images were recorded at 5x5µm, and surface roughness (Ra) was calculated. The analysis was performed on at least three randomly selected regions per film.

2.3.2. Optical Microscopy

The Optical microscopy Olympus FV1000 (confocal) was used to examine the general morphology and homogeneity of the films. The polymer films were placed under the optical microscope at various magnifications using objective lens from 5x to 100x. The images captured shows nanoparticle dispersion and clusters within certain regions of polymer matrix which is a tendency for phase separation

2.3.3. Fourier Transform Infrared Spectroscopy (FTIR)

A sample of each polymer film was placed on the FTIR instrument, and the machine was set at baseline with blank sample. The instrument passed infrared lights through the samples, and the spectrum was recorded based on the absorption of different wavelengths from 4000 to 400cm-1. Further analysis was done on the characterization peak of the resulting spectrum which corresponds to the functional group of HA and Zn

2.3.4. Mechanical Properties (Tensile Strength)

Tensile testing of samples of the resulting composite polymer material was carried out according to the requirements on an Instron 5943 testing machine.The test method complies with the requirements of GOST 14236-81 (ST SEV 1490-79) "Polymer films. Tensile test method."; GOST 11262-2017 (ISO 527-2:2012) "Plastics. Tensile test method." and ASTM D882-18 "Standard Test Method for Tensile Properties of Thin Plastic Sheeting".The Test specimens were prepared in compliance with the requirements of GOST 12423-2013 (ISO 291:2008) “Plastics. Conditions for conditioning and testing (samples).The various samples of thin film was cut into stripes of equal length and breadth of 5cm by 1 cm respectively and the thickness was measured using a digital micrometer. Each film was cut into 5 to 6 pieces of stripes and measured separately. The measured thickness was taken within the 3mm range from the middle to both end for each stripes in a film and the average thickness was recorded

FTIR Analysis

Fourier Transform infrared (FTIR) spectroscopy was used to identify the functional groups and to evaluate molecular reactions between the polymer and nanoparticles that forms the composite (HA_ZnO) and to record other components. This analysis identifies the chemical bonding, crosslinking and interfacial compatibility within the Polymer matrix.

The spectra were recorded using Bruker Alpha II FTIR spectrometer (Bruker Optics Germany) which is equipped with attenuated total reflectance (ATR) accessory containing a diamond/ZnSe crystal. Spectra were measured within the wavenumber range of 4000-400cm^{-1} at a resolution of 4cm^{-1} and an average of 50 scans per sample was measured to improve the signal to noise ratio. Moreso, before the experimental analysis, the background spectrum ws obtained under similar conditions.

3. Results

3.1. Optimization of ZnO NPs in HA Composite Film

Various concentrations of ZnO were prepared for the composite film formation to optimize it. Solution concentration of 0,1,3,5 7 and 10 % (w/w relative to HA) were prepared and cast for drying

© 2025 by the author(s). Distributed under a Creative Commons CC BY license.

Preprints.org (www.preprints.org) | NOT PEER-REVIEWED | Posted: 10 November 2025 doi:10.20944/preprints202511.0609.v1

using similar parameters of temperature, mixing speed and relative humidity. This will enable the evaluation of influence of nanoparticles loading on film microstructure by using AFM and mechanical analysis (Tensile strength and elongation at break). Figure 4 a-d shows the composite film morphology and Table 2 shows a summary of the mechanical properties and film thickness. The 2% HA only (5a), displayed a relatively smooth sheen surface, while towards 5%ZnO (5b) there is a fine dispersion and moderate surface roughness. A further increase in ZnO concentration towards 7% (5c) and 10% (5d)shows a significant cluster formation and agglomeration and phase separation which leads to an uneven surface structure and compromised film integrity.

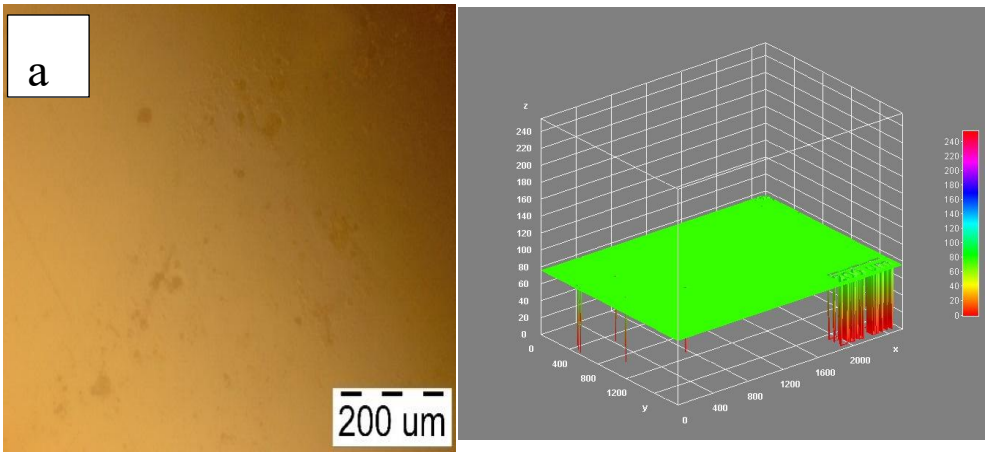

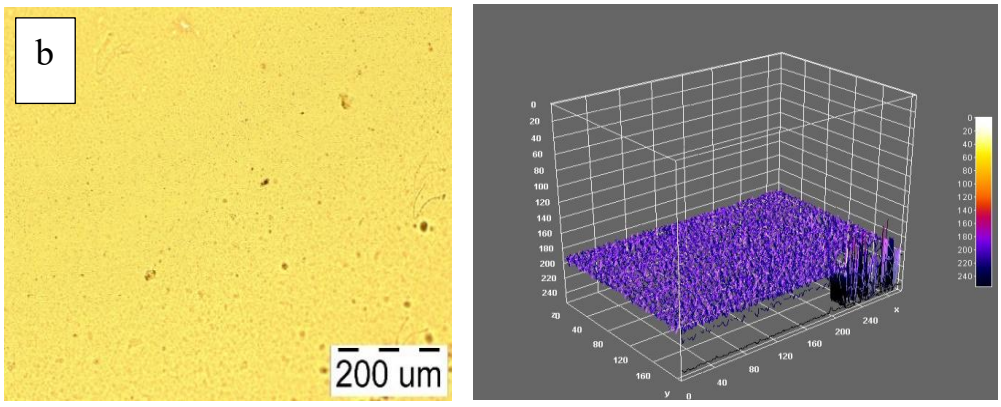

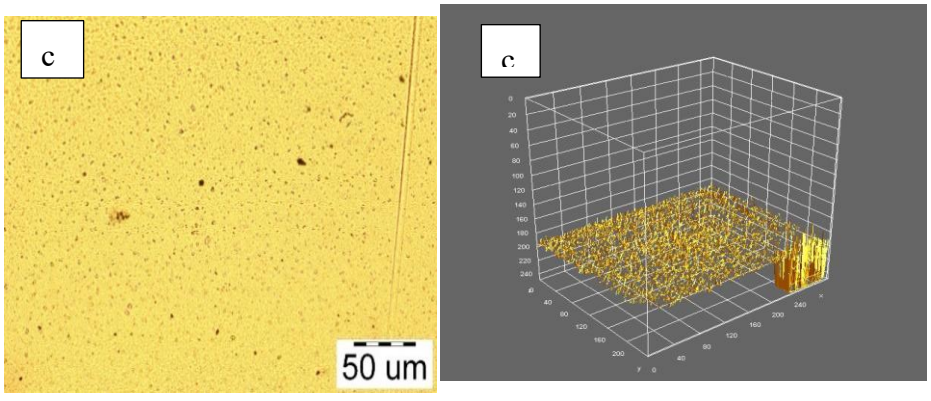

© 2025 by the author(s). Distributed under a Creative Commons CC BY license.

Preprints.org (www.preprints.org) | NOT PEER-REVIEWED | Posted: 10 November 2025 doi:10.20944/preprints202511.0609.v1

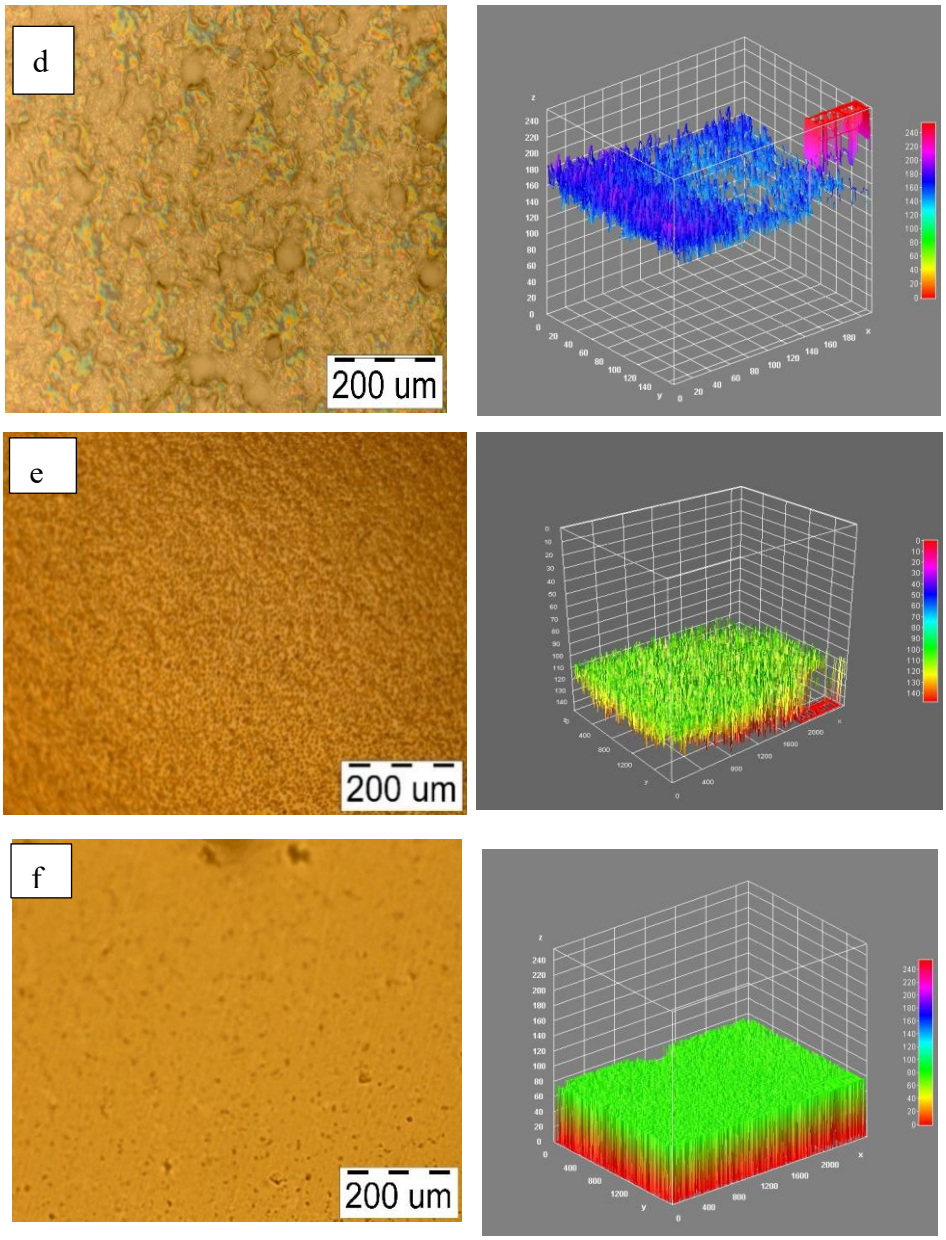

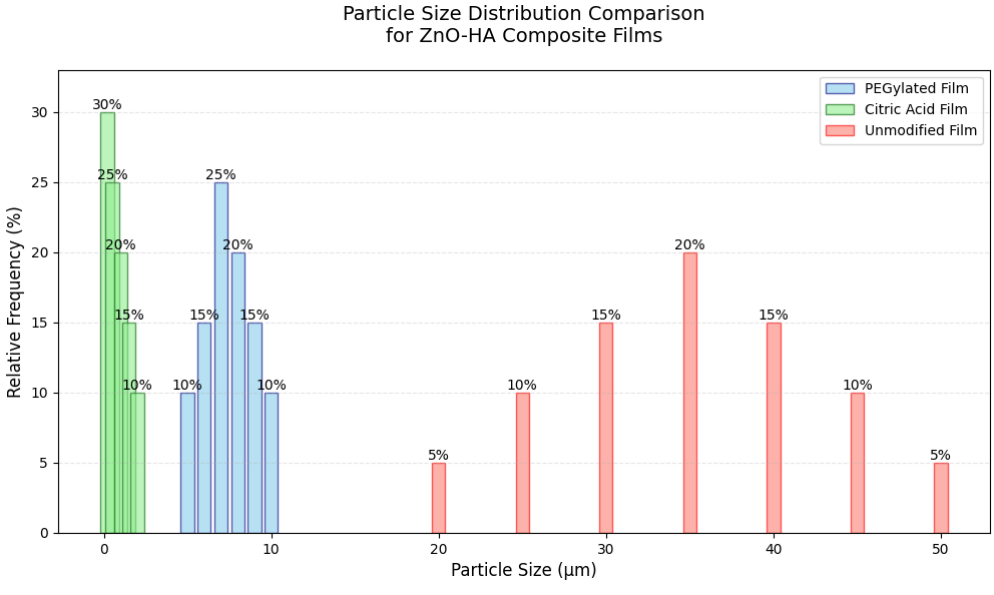

(g)

© 2025 by the author(s). Distributed under a Creative Commons CC BY license.

Preprints.org (www.preprints.org) | NOT PEER-REVIEWED | Posted: 10 November 2025 doi:10.20944/preprints202511.0609.v1

Figure 4. (a-f) shows Optical microscope images of HA composite films with varying concentration and surface modification (a) 2% HA only; (b) 5% ZnO; (c) 7% ZnO; (d) 10% ZnO; (e) 10% ZnO PEGylation (f) 10% ZnO citric acid chelation. The 5%ZnO film shows significant homogenous dispersion whereas (7% and 10%) display nanoparticle clustering and aggregation. PEGylating and chelation treatments improve uniformity and colloidal stability of selected 10% ZnO films. Scale bar 200µm while 1 (c) is scaled to 50 µm. (g) *shows* particle size distribution comparison for composite films modified (HA_ZnO10%_PEG and HA_Zn010%_CA) and unmodified ZnO 10%.

Composition	Property	Trial1	Trial2	Trial3	Mean ±SD	± %Error
HA0,2% only	Thickness(mm)	0,0110	0,0120	0,0130	0,012 ±0,001	± 8%
	Tensile (Mpa)	6,921	7,690	8,459	7,69 ±0,77	± 10%
	Elongation (%)	3,71	4,22	4,73	4,22 ± 0,51	± 12 %
	Young Modulus (Mpa)	130,73	145,26	159,79	145,26 ±14,53	± 10 %
Composition	**Property**	**Trial1**	**Trial2**	**Trial3**	**Mean ±SD**	**± %Error**
HA+ZnO 1%	Thickness(mm)	0,0166	0,0180	0,0194	0,018 ±0,001	± 8%
	Tensile (Mpa)	26,34	29,27	32,20	29,27 ±2,93	± 10%
	Elongation (%)	7,46	8,47	9,48	8,47 ± 1,02	± 12 %
	Young Modulus (Mpa)	677,70	753,00	828,30	753,00 ±75,30	± 10 %
Composition	**Property**	**Trial1**	**Trial2**	**Trial3**	**Mean ±SD**	**± %Error**
HA+ZnO 3%	Thickness(mm)	0,0267	0,0290	0,0313	0,029 ±0,002	± 8%
	Tensile (Mpa)	21,26	23,62	25,98	23,62 ±2,36	± 10%
	Elongation (%)	4,01	4,56	5,11	4,56 ± 0,61	± 12 %
	Young Modulus (Mpa)	1110,42	1233,80	1357,18	1233,80±123,38	± 10 %

Composition	**Property**	**Trial1**	**Trial2**	**Trial3**	**Mean ±SD**	**± %Error**
HA+ZnO 5%	Thickness(mm)	0,0202	0,0220	0,0238	0,022 ±0,002	± 8%
	Tensile (Mpa)	23,09	25,66	28,23	25,66 ±2,57	± 10%
	Elongation (%)	7,29	8,29	9,29	8,29 ± 1,00	± 12 %
	Young Modulus (Mpa)	838,67	931,85	1025,04	931,85±93,19	± 10 %
Composition	**Property**	**Trial1**	**Trial2**	**Trial3**	**Mean ±SD**	**± %Error**
HA+ZnO 7%	Thickness(mm)	0,0230	0,0250	0,0270	0,025 ±0,002	± 8%
	Tensile (Mpa)	4,41	4,90	5,39	4,90 ±0,49	± 10%
	Elongation (%)	9,89	11,23	12,57	11,23 ± 1,34	± 12 %

© 2025 by the author(s). Distributed under a Creative Commons CC BY license.

Preprints.org (www.preprints.org) | NOT PEER-REVIEWED | Posted: 10 November 2025 doi:10.20944/preprints202511.0609.v1

	Young Modulus (Mpa)	529,53	588,37	647,21	588,37±58,84	± 10 %
Composition	**Property**	**Trial1**	**Trial2**	**Trial3**	**Mean ±SD**	**± %Error**
HA+ZnO 10%	Thickness(mm)	0,0377	0,0410	0,0443	0,041 ±0,003	± 8%
	Tensile (Mpa)	15,17	17,44	19,18	17,44 ±1,74	± 10%
	Elongation (%)	8,32	9,43	10,54	9,43 ± 1,11	± 12 %
	Young Modulus (Mpa)	859,70	955,22	1050,74	955,22±95,52	± 10 %

At lower concentration of ZnO between 1-3% shows a steady improvement of Tensile strength in relation to HA films, good dispersion and effective interfacial bonding. There is also a restriction of polymer chain mobility due to the homogeneous dispersion of nanoparticles which leads to stiffer and flexible microstructure composite film. The moment the ZnO concentration is increased to 5-7%, there is a reduction in tensile strength and elongation. The decline in these mechanical properties is because of possible cluster formation which is optimized at 5% concentration. This depicts local particles to particle interaction rather than bonding with polymer chain, hereby reducing stress transfer efficiency.

Finally, at increased in ZnO concentration to 10%, there is a decrease in Tensile strength and elongation at break which confirms phase separations uneven distribution of ZnO, forms cluster and creates a weak point under tensile loading.

Mechanical testing revealed that 5% ZnO film is the optimized composite film based on parameters of formation as it creates balance between tensile strength and elongation at break. The higher concentration reduces flexibility and brittleness due to ZnO clusters

3.2. PEGylation and Chelation on Colloidal Stability and Microstructure

While evaluating and optimizing at 5% concentration ZnO, further analysis was conducted from the optimized concentration to 10 %ZnO of the composite film. The preparation procedure was followed as before but this time the prepared solution of ZnO was subjected to PEGylation and citric acid chelation. FM and Optical microscope were used to study film morphology and mechanical properties as demonstrated in Figure 5e-f the Table 3 below and Figure 4. The results show that PEGylation was able to improve dispersion and reduce surface roughness, while chelation stabilized ZnO particles by coordinating with surface Zn^{2+} ions. The two modification processes as explained enhanced the composite film uniformity and minimized phase separation compared to unmodified version.

© 2025 by the author(s). Distributed under a Creative Commons CC BY license.

Preprints.org (www.preprints.org) | NOT PEER-REVIEWED | Posted: 10 November 2025 doi:10.20944/preprints202511.0609.v1

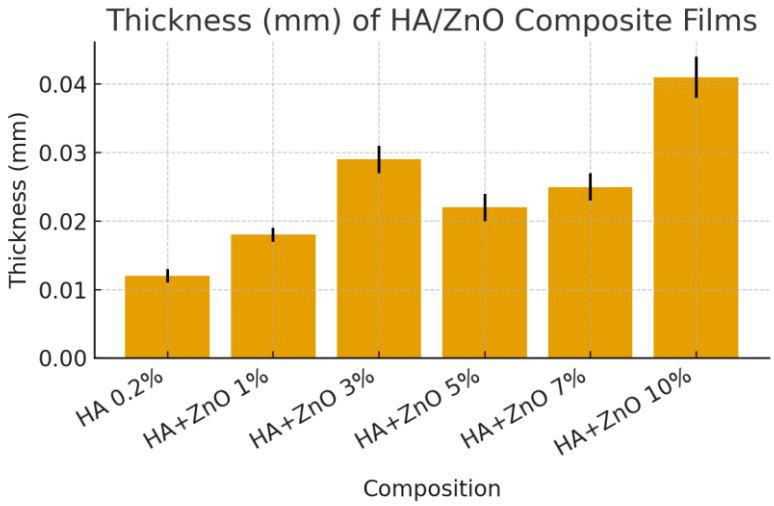

Fig 5 (a)

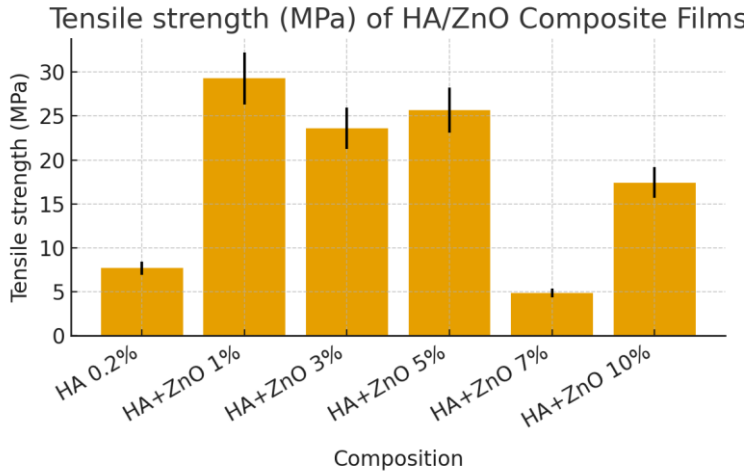

Fig 5 (b)

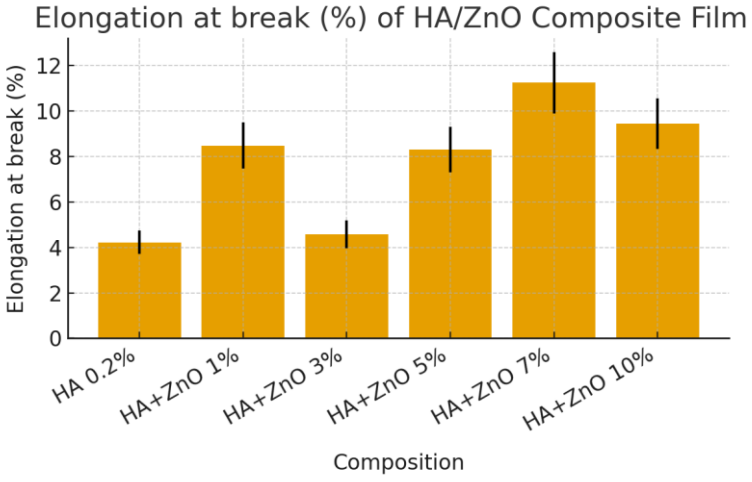

Fig 5 (c)

© 2025 by the author(s). Distributed under a Creative Commons CC BY license.

Preprints.org (www.preprints.org) | NOT PEER-REVIEWED | Posted: 10 November 2025 doi:10.20944/preprints202511.0609.v1

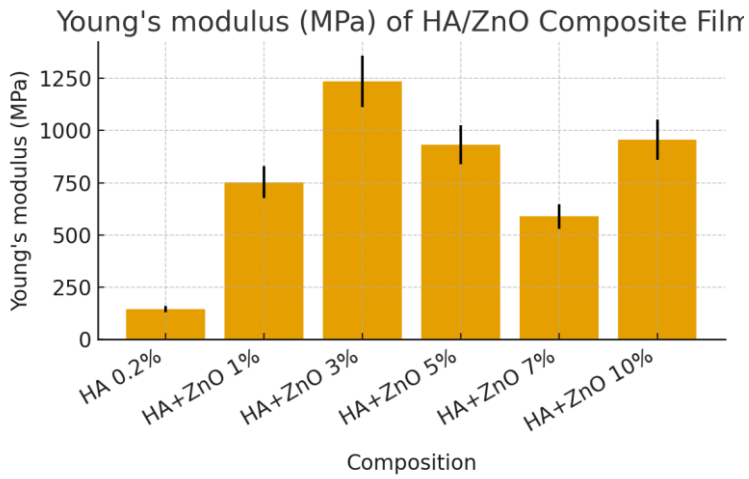

Fig 5 (d)

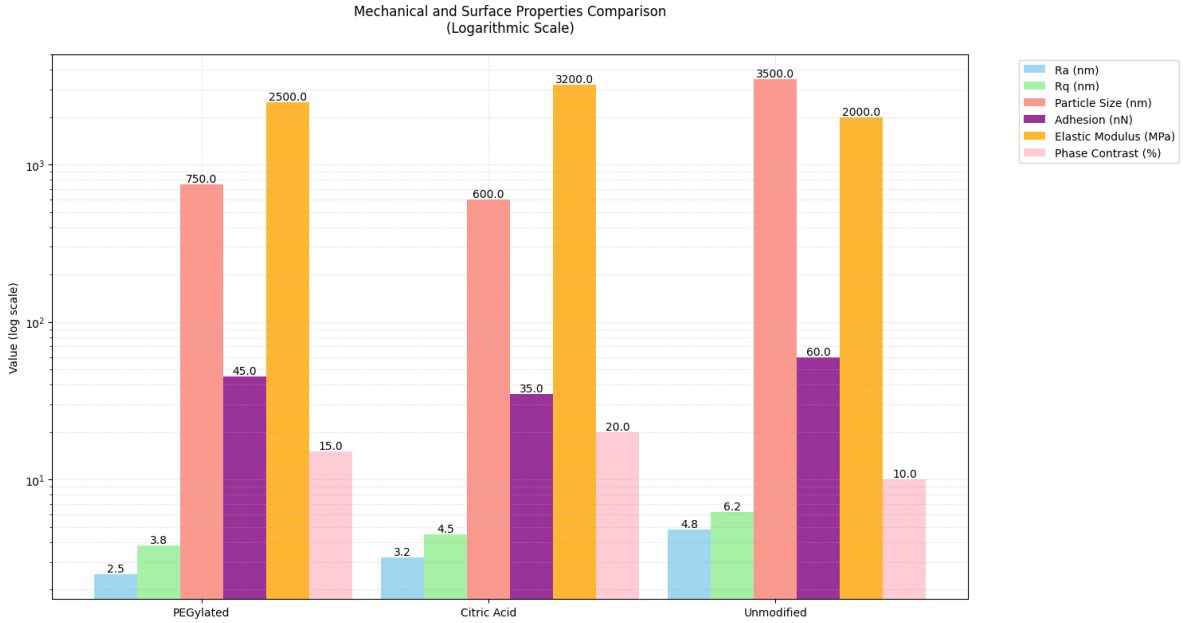

Figure 5. (a-d) The histogram and error bar depicts that the increment in ZnO concentration in the HA matrix directly influences the thickness, Mechanical properties such as Tensile strength, young modulus and elongation at break.

Table 3. AFM DATA.

Parameters	0%ZnO(Pure HA)	PEGylated ZnO10%	Chelating agent+ ZnO10%	Unmodified ZnO10%
Surface roughness (Ra,nm)	2,0 ± 0,3	2,5 ± 0,3	3,2 ± 0,3	4,8 ± 0,3
RMS Roughness(Rq,nm)	3,0 ± 0,4	3,8 ± 0,4	4,5 ± 0,4	6,2 ± 0,4
Particle size (nm)	N/A	750 ± 12	600 ± 12	3500 ± 12
Adhesion Force(nN)	15,0 ± 2,1	45,0 ± 2,1	35,0 ± 2,1	60,0 ± 2,1
Elastic Modulus(Mpa)	150 ± 15	2500 ± 15	3200 ± 15	2000 ± 15

© 2025 by the author(s). Distributed under a Creative Commons CC BY license.

Preprints.org (www.preprints.org) | NOT PEER-REVIEWED | Posted: 10 November 2025 doi:10.20944/preprints202511.0609.v1

Phase Contrast δPhase,%)	8 ± 1	15 ± 1	20 ± 1	10 ± 1

Figure 6 shows the mechanical and surface properties comparison for PEGylated, chelation and unmodified surface of ZnO in the polymer matrix

3.3. Microstructure and Mechanical Performance Evaluation

Here we demonstrated surface chemistry as a tool to fine-tune both structural and functional properties of the composite films. The relativity of microstructure and mechanical performance was evaluated, using the nanoparticle dispersion in the 5%ZnO-10% for analysis. Starting with the Optimal ZnO5% concentration, a trend of balanced tensile strength and flexibility was observed. PEGylation and chelation helped to improve the interfacial compatibility and colloidal stability. The study of the combined analysis of AFM images, mechanical data and phase behavior reflects the importance of selecting the right concentration and surface treatment to achieve uniform films across surface areas with predictable mechanical and colloidal properties.

in this section. If there is no role, please state "The funders had no role in the design of the study; in the collection, analyses, or interpretation of data; in the writing of the manuscript; or in the decision to publish the results".

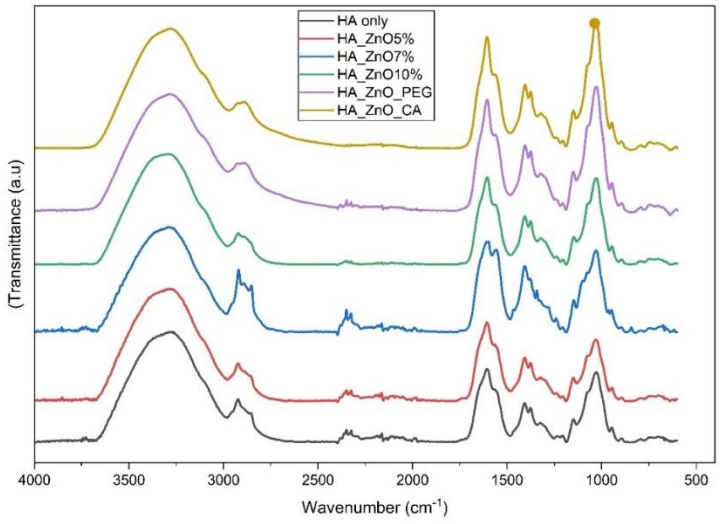

Figure 7. Shows FTIR analysis graph for composite films as labelled on the graph.where HA_ZnO_PEG.

The FTIR analysis in Table 4 displays the microstructural analysis through peak readings for each sample of film ranging from 0 to 10% ZnO concentration and the modified composite film using PEG (Polyethylene glycol) and CA (citric acid).The indications of available parameters suggests that there is a good interfacial compatibility up to 5%ZnO concentration which slightly reaches its optimal at 7%ZnO as it shows strongest peak intensity. At 10%ZnO concentration, it begins to display phase separation as peak broadening is observed in the spectra. The PEGylated composite film shows additional functional group and enhanced compatibility, likewise the CA chelating agent confirms improved compatibility due to distinct peak shift. The induced phase separation and weak interfacial interaction show a possible reduction and degradation of the mechanical properties of the composite, especially at high ZnO concentrations

Table 4. Wavenumber Analysis.

© 2025 by the author(s). Distributed under a Creative Commons CC BY license.

Preprints.org (www.preprints.org) | NOT PEER-REVIEWED | Posted: 10 November 2025 doi:10.20944/preprints202511.0609.v1

Wavenumber range cm^{-1}	Functional group	Peak characteristics	Compatibility Evidence	Effect of modification
3500-3550	O-H stretching	Sharp peaks 0-7%ZnO	Peak broadening at 10%ZnO	Enhanced peak intensity PEG/CA
2850-3000	C-H stretching	Progressive intensity increases to 7%	Reduced intensity at 10%	Additional absorption bands
17003	C=O stretching	Max. intensity at 7%ZnO	Peak shift in modified composites	Distinct peak shift in PEG/CA
33001	N-H stretching	Clear transition at 0-7%	Peak broadening at 10%	Enhanced peak definition
1550-1650	N-H Bending	Sharp peaks 0-7%	Reduced intensity at 10%	Increased peak intensity

Modern imaging techniques have proved extremely useful over traditional methods, for observing the microstructural characteristics of composite materials, that provides the basis for future research objectively focused on developing the properties of HA-ZnO nanocomposites for biomedical and industrial applications.

4. Conclusion

The findings show consistency in literature reviews where ZnO concentration has significant impact in composite structure, where optimal values are obtained at lower ZnO concentration in most composites' formulation. The phase separation and weak interfacial interaction of molecules due to high ZnO concentration is one of the fundamental challenges in nanocomposites synthesis and its effectiveness in drug delivery behavior. Further research suggests the surface modification of ZnO using polymers like PEG or chelating agent can proffer a solution for interfacial compatibility. The characterization of these nano composites materials using modern imaging techniques will provide more valuable results for future optimization. The research contributes to the understanding of optimal formulation parameters in concentration control for balance in interfacial compatibility for desired material properties in wound dressing, drug delivery and tissue engineering in the aspect of scaffold prototype design for cell proliferation.

The studying of the surface morphology of the composite film was examined using Image J software to understand the particle distribution,phase separation and interfacial uniformity. Scanning Electron microscope (SEM) can also be employed to study the morphology but the combination of optical microscopy and Image J shows a reliable means of visualizing the film microstructure under either hydrated or partically hydrated conditions which demonstrates it potentials for routine evaluation of biopolymer, especially in the absence of SEM availability.This approach does not only confirmed the presence of phase seperation but also demonstrates that optical tools can be used for characterization of film morphology.

Author: Contributions Conceptualization, Kolawole S. Dada. and Roman O. Olekhnovich..; methodology, Roman O. Olekhnovich...; validation, Roman O. Olekhnovich...; formal analysis, Kolawole S. Dada and Falia F. Zaripova ; investigation, Kolawole S. Dada.; resources, Kolawole S. Dada.; data curation, Kolawole S. Dada.; writing—original draft preparation, Kolawole S. Dada.; writing—review and editing, Kolawole S. Dada.; visualization, Kolawole S. Dada.; supervision, , Roman O. Olekhnovich.; project administration, Roman O. Olekhnovich..;. All authors have read and agreed to the published version of the manuscript.

© 2025 by the author(s). Distributed under a Creative Commons CC BY license.

Preprints.org (www.preprints.org) | NOT PEER-REVIEWED | Posted: 10 November 2025 doi:10.20944/preprints202511.0609.v1

Funding: This research received no external funding.

Institutional Review Board Statement: Not applicable.

Data Availability Statement: Data are available upon request .

Conflicts of Interest: Declare conflicts of interest or state "The authors declare no conflicts of interest.

References

1. C. Buckley, E. J. Murphy, T. R. Montgomery, and I. Major, "Hyaluronic Acid: A Review of the Drug Delivery Capabilities of This Naturally Occurring Polysaccharide," *Polymers (Basel)*, vol. 14, no. 17, p. 3442, Aug. 2022, doi: 10.3390/polym14173442.
2. A. Yasin, Y. Ren, J. Li, Y. Sheng, C. Cao, and K. Zhang, "Advances in Hyaluronic Acid for Biomedical Applications," *Front Bioeng Biotechnol*, vol. 10, Jul. 2022, doi: 10.3389/fbioe.2022.910290.
3. A. S *et al.*, "Harnessing natural polymers and nanoparticles: Synergistic scaffold design for improved wound healing," *Hybrid Advances*, vol. 8, p. 100381, Mar. 2025, doi: 10.1016/j.hybadv.2025.100381.
4. Y. Zare, "Study of nanoparticles aggregation/agglomeration in polymer particulate nanocomposites by mechanical properties," *Compos Part A Appl Sci Manuf*, vol. 84, pp. 158–164, May 2016, doi: 10.1016/j.compositesa.2016.01.020.
5. A. E. Nel *et al.*, "Understanding biophysicochemical interactions at the nano–bio interface," *Nat Mater*, vol. 8, no. 7, pp. 543–557, Jul. 2009, doi: 10.1038/nmat2442.
6. D. Kesler, B. P. Ariyawansa, and H. Rathnayake, "Mechanical Properties and Synergistic Interfacial Interactions of ZnO Nanorod-Reinforced Polyamide–Imide Composites," *Polymers (Basel)*, vol. 15, no. 6, p. 1522, Mar. 2023, doi: 10.3390/polym15061522.
7. R. Alipoor, M. Ayan, M. R. Hamblin, R. Ranjbar, and S. Rashki, "Hyaluronic Acid-Based Nanomaterials as a New Approach to the Treatment and Prevention of Bacterial Infections," *Front Bioeng Biotechnol*, vol. 10, Jun. 2022, doi: 10.3389/fbioe.2022.913912.
8. A. N. Bokatyi, N. V. Dubashynskaya, and Y. A. Skorik, "Chemical modification of hyaluronic acid as a strategy for the development of advanced drug delivery systems," *Carbohydr Polym*, vol. 337, p. 122145, Aug. 2024, doi: 10.1016/j.carbpol.2024.122145.
9. A. Maleki, A. Kjøniksen, and B. Nyström, "Effect of pH on the Behavior of Hyaluronic Acid in Dilute and Semidilute Aqueous Solutions," *Macromol Symp*, vol. 274, no. 1, pp. 131–140, Dec. 2008, doi: 10.1002/masy.200851418.
10. A. Fallacara, E. Baldini, S. Manfredini, and S. Vertuani, "Hyaluronic Acid in the Third Millennium," *Polymers (Basel)*, vol. 10, no. 7, p. 701, Jun. 2018, doi: 10.3390/polym10070701.
11. K. S. Dada, M. V. Uspenskaya, C. N. Elangwe, A. O. Nosova, and R. O. Olekhnovich, "Exploring the influence of mechanical and physical characteristics on transdermal patches: A study on polymeric films composed of hyaluronic acid and zinc oxide nanoparticles," *Proceedings of the Voronezh State University of Engineering Technologies*, vol. 86, no. 3, pp. 282–288, Dec. 2024, doi: 10.20914/2310-1202-2024-3-282-288.
12. S.-P. Rwei, S.-W. Chen, C.-F. Mao, and H.-W. Fang, "Viscoelasticity and wearability of hyaluronate solutions," *Biochem Eng J*, vol. 40, no. 2, pp. 211–217, Jun. 2008, doi: 10.1016/j.bej.2007.12.021.
13. A. Sionkowska, M. Gadomska, K. Musiał, and J. Piątek, "Hyaluronic Acid as a Component of Natural Polymer Blends for Biomedical Applications: A Review," *Molecules*, vol. 25, no. 18, p. 4035, Sep. 2020, doi: 10.3390/molecules25184035.
14. M. Khaleghi, E. Ahmadi, M. Khodabandeh Shahraki, F. Aliakbari, and D. Morshedi, "Temperature-dependent formulation of a hydrogel based on Hyaluronic acid-polydimethylsiloxane for biomedical applications," *Heliyon*, vol. 6, no. 3, p. e03494, Mar. 2020, doi: 10.1016/j.heliyon.2020.e03494.
15. V. Hintze, M. Schnabelrauch, and S. Rother, "Chemical Modification of Hyaluronan and Their Biomedical Applications.," *Front Chem*, vol. 10, p. 830671, 2022, doi: 10.3389/fchem.2022.830671.
16. N. Petit, Y. J. Chang, F. A. Lobianco, T. Hodgkinson, and S. Browne, "Hyaluronic acid as a versatile building block for the development of biofunctional hydrogels: In vitro models and preclinical innovations," *Mater Today Bio*, vol. 31, p. 101596, Apr. 2025, doi: 10.1016/j.mtbio.2025.101596.

© 2025 by the author(s). Distributed under a Creative Commons CC BY license.

Preprints.org (www.preprints.org) | NOT PEER-REVIEWED | Posted: 10 November 2025 doi:10.20944/preprints202511.0609.v1

17. A. Khorsand Zak, W. H. Abd. Majid, M. E. Abrishami, and R. Yousefi, "X-ray analysis of ZnO nanoparticles by Williamson–Hall and size–strain plot methods," *Solid State Sci*, vol. 13, no. 1, pp. 251–256, Jan. 2011, doi: 10.1016/j.solidstatesciences.2010.11.024.
18. R. Rohani, N. S. F. Dzulkharnien, N. H. Harun, and I. A. Ilias, "Green Approaches, Potentials, and Applications of Zinc Oxide Nanoparticles in Surface Coatings and Films," *Bioinorg Chem Appl*, vol. 2022, no. 1, Jan. 2022, doi: 10.1155/2022/3077747.
19. S. N. Zailan, A. Bouaissi, N. Mahmed, and M. M. A. B. Abdullah, "Influence of ZnO Nanoparticles on Mechanical Properties and Photocatalytic Activity of Self-cleaning ZnO-Based Geopolymer Paste," *J Inorg Organomet Polym Mater*, vol. 30, no. 6, pp. 2007–2016, Jun. 2020, doi: 10.1007/s10904-019-01399-3.
20. A. U. H. Khan *et al.*, "Changes in the Aggregation Behaviour of Zinc Oxide Nanoparticles Influenced by Perfluorooctanoic Acid, Salts, and Humic Acid in Simulated Waters," *Toxics*, vol. 12, no. 8, p. 602, Aug. 2024, doi: 10.3390/toxics12080602.
21. S. Thipperudrappa, A. Ullal Kini, and A. Hiremath, "Influence of zinc oxide nanoparticles on the mechanical and thermal responses of glass fiber-reinforced epoxy nanocomposites," *Polym Compos*, vol. 41, no. 1, pp. 174–181, Jan. 2020, doi: 10.1002/pc.25357.
22. T. F. Moghadam and S. Azizian, "Effect of ZnO nanoparticles on the interfacial behavior of anionic surfactant at liquid/liquid interfaces," *Colloids Surf A Physicochem Eng Asp*, vol. 457, pp. 333–339, Sep. 2014, doi: 10.1016/j.colsurfa.2014.06.009.
23. K. S. Siddiqi, A. ur Rahman, Tajuddin, and A. Husen, "Properties of Zinc Oxide Nanoparticles and Their Activity Against Microbes," *Nanoscale Res Lett*, vol. 13, no. 1, p. 141, Dec. 2018, doi: 10.1186/s11671-018-2532-3.
24. S. Shankar, L.-F. Wang, and J.-W. Rhim, "Incorporation of zinc oxide nanoparticles improved the mechanical, water vapor barrier, UV-light barrier, and antibacterial properties of PLA-based nanocomposite films," *Materials Science and Engineering: C*, vol. 93, pp. 289–298, Dec. 2018, doi: 10.1016/j.msec.2018.08.002.
25. D. K. Sharma, S. Shukla, K. K. Sharma, and V. Kumar, "A review on ZnO: Fundamental properties and applications," *Mater Today Proc*, vol. 49, pp. 3028–3035, 2022, doi: 10.1016/j.matpr.2020.10.238.
26. S. Anjum *et al.*, "Recent Advances in Zinc Oxide Nanoparticles (ZnO NPs) for Cancer Diagnosis, Target Drug Delivery, and Treatment.," *Cancers (Basel)*, vol. 13, no. 18, Sep. 2021, doi: 10.3390/cancers13184570.
27. L. Racca *et al.*, "Zinc Oxide Nanostructures in Biomedicine," in *Smart Nanoparticles for Biomedicine*, Elsevier, 2018, pp. 171–187. doi: 10.1016/B978-0-12-814156-4.00012-4.
28. A. M. Juncan *et al.*, "Advantages of Hyaluronic Acid and Its Combination with Other Bioactive Ingredients in Cosmeceuticals," *Molecules*, vol. 26, no. 15, p. 4429, Jul. 2021, doi: 10.3390/molecules26154429.
29. G. T. Balogh, J. Illés, Z. Székely, E. Forrai, and A. Gere, "Effect of different metal ions on the oxidative damage and antioxidant capacity of hyaluronic acid," *Arch Biochem Biophys*, vol. 410, no. 1, pp. 76–82, Feb. 2003, doi: 10.1016/S0003-9861(02)00661-6.
30. U. T. Uthappa, M. Suneetha, K. V Ajeya, and S. M. Ji, "Hyaluronic Acid Modified Metal Nanoparticles and Their Derived Substituents for Cancer Therapy: A Review.," *Pharmaceutics*, vol. 15, no. 6, Jun. 2023, doi: 10.3390/pharmaceutics15061713.
31. S. L. Chia and D. T. Leong, "Reducing ZnO nanoparticles toxicity through silica coating," *Heliyon*, vol. 2, no. 10, p. e00177, Oct. 2016, doi: 10.1016/j.heliyon.2016.e00177.
32. J. Sahoo, S. Sarkhel, N. Mukherjee, and A. Jaiswal, "Nanomaterial-Based Antimicrobial Coating for Biomedical Implants: New Age Solution for Biofilm-Associated Infections," *ACS Omega*, vol. 7, no. 50, pp. 45962–45980, Dec. 2022, doi: 10.1021/acsomega.2c06211.
33. N. Jayaprakash, K. Elumalai, S. Manickam, G. Bakthavatchalam, and P. Tamilselvan, "Carbon nanomaterials: Revolutionizing biomedical applications with promising potential," *Nano Materials Science*, Dec. 2024, doi: 10.1016/j.nanoms.2024.11.004.
34. C. Cha, S. R. Shin, N. Annabi, M. R. Dokmeci, and A. Khademhosseini, "Carbon-Based Nanomaterials: Multifunctional Materials for Biomedical Engineering," *ACS Nano*, vol. 7, no. 4, pp. 2891–2897, Apr. 2013, doi: 10.1021/nn401196a.

© 2025 by the author(s). Distributed under a Creative Commons CC BY license.

Preprints.org (www.preprints.org) | NOT PEER-REVIEWED | Posted: 10 November 2025 doi:10.20944/preprints202511.0609.v1

35. K. S. Dada, M. V. Uspenskaya, C. N. Elangwe, A. O. Nosova, and R. O. Olekhnovich, "Exploring the influence of mechanical and physical characteristics on transdermal patches: A study on polymeric films composed of hyaluronic acid and zinc oxide nanoparticles," *Proceedings of the Voronezh State University of Engineering Technologies*, vol. 86, no. 3, pp. 282–288, Dec. 2024, doi: 10.20914/2310-1202-2024-3-282-288.

Disclaimer/Publisher's Note: The statements, opinions and data contained in all publications are solely those of the individual author(s) and contributor(s) and not of MDPI and/or the editor(s). MDPI and/or the editor(s) disclaim responsibility for any injury to people or property resulting from any ideas, methods, instructions or products referred to in the content.

© 2025 by the author(s). Distributed under a Creative Commons CC BY license.